Observing atmospheric gravity waves from the Space Station

Dana L. McGuffin
Lawrence Livermore National Laboratory
Hassan Beydoun
Lawrence Livermore National Laboratory

Scott A. Budzien
Naval Research Laboratory, Washington D.C.,

Philip J. Cameron-Smith
Lawrence Livermore National Laboratory

Kenneth F. Dymond
Naval Research Laboratory, Washington D.C.

Matthew A. Horsley
Lawrence Livermore National Laboratory

Katherine A. Zawdie
Naval Research Laboratory, Washington D.C., USA

ABSTRACT

Small-scale atmospheric gravity waves (GWs) are deviations in atmospheric density that transport momentum throughout the atmosphere. Stratospheric winds are accelerated as GWs dissipate to turbulence, but the intensity and altitude of GW breaking is uncertain. Gravity waves, and the turbulence they produce, are difficult to observe from the ground and are currently not well characterized. Four different instruments able to observe GWs are joining the suite of instruments on the International Space Station (ISS): ECLIPSE, VvIPRE, SOHIP, and AWE. In this work, we utilize atmospheric and space weather models to provide synthetic data to assess the ability of these four instruments to observe GWs propagating from the troposphere to ionosphere. This analysis shows that SOHIP, ECLIPSE, and AWE can observe GW propagation characteristics. The preliminary spectral analysis of the simulated measurements estimate vertical wavelengths 2 km to 3 km in the stratosphere and roughly 100 km in the thermosphere as well as horizontal wavelengths from 250 km to 1,000 km in the mesosphere. Future work should utilize 2-dimensional spectral analysis for estimates of horizontal wavelengths and propagation direction. Combining these datasets to observe the GW field spectral, spatial, and temporal characteristics can provide useful information for communication and navigation systems.

1. INTRODUCTION

Small-scale atmospheric gravity waves (GWs), which are formed due to topography (i.e. mountains), convection, or strong wind jets, transport energy and momentum across long distances with wavelengths from tens to hundreds of km. GWs propagate until they reach instability, break, and generate turbulence on the scale of 10 km to diffusion length scales (below 1 m). GWs drive high altitude weather phenomena with deviations in atmospheric density and turbulence that accelerate stratospheric winds, producing the mean circulation, Quasi Biennial Oscillation (QBO), and breakdown of the polar vortex. Therefore, to develop a comprehensive understanding of the behavior of the upper

atmosphere, it is vital to observe and understand these upper atmospheric gravity waves. However, gravity waves, and the turbulence they produce, are difficult to observe from the ground and are currently not well characterized.

Four different instruments able to observe GWs are joining the suite of instruments on the International Space Station (ISS). The Experiment for Characterizing Lower Ionosphere & Production of Sporadic-E (ECLIPSE) measures both horizontal and vertical profiles of electron and ion density between 60 km to 400 km altitude. The Variable Voltage Ion Protection Experiment (VVIPRE) measures the vertical profile of electron and ion density at a 10 km resolution. The Stellar Occultation Hypertemporal Imaging Payload (SOHIP) measures atmospheric refraction soundings from 10 km to 60 km altitudes at 10 m vertical resolution via stellar occultation. With a high vertical resolution, SOHIP measures turbulence via stellar scintillation in addition to vertical GW via stellar refraction. ECLIPSE, VvIPRE, and SOHIP launched to the ISS on the same payload with the Space Test Program in March 2023. The Atmospheric Waves Experiment (AWE) is planned to launch in late 2023 to measure the airglow temperature observing the nighttime hydroxyl emission.

In this work, we investigate whether measurements from these four different satellite-based instruments can be combined to observe GWs propagating from the troposphere to ionosphere. We will show a case study with simulated measurements of convective GWs from each of the instruments. The lower atmospheric simulation models a strong convective system forming GWs with the Weather Research & Forecasting (WRF) model from the surface to 60 km altitude. The upper atmospheric simulation models the medium-scale traveling ionospheric disturbances with the SAMI3 numerical model (Sami3 is Also a Model of the Ionosphere) based on lower atmospheric boundary conditions from a strong convective storm.

The simulated data is sampled based on the instrument viewing geometries from the ISS, and the spatial resolution is based on the instrument operating parameters. Additionally, the instruments measure different properties of the atmosphere. While SOHIP and AWE observe temperature, ECLIPSE and VVIPRE observe ion densities. Therefore, each instrument has a different sensitivity to GWs, which must be considered when performing data fusion and assimilation into models.

We will discuss the feasibility of observing upper atmosphere disturbances with these new satellite observations. The diverse spatial resolution, quantities measured, and viewing geometries among the four instruments can provide a more complete understanding of GWs than one measurement alone.

2. INSTRUMENTS ON THE SPACE STATION

The ISS instruments have potential to observe smaller scale gravity waves than previously measured. However, the remote measurements observe different slices of the atmosphere with VvIPRE and ECLIPSE targeting the thermosphere and ionosphere, AWE targeting the mesosphere, and SOHIP targeting the stratosphere. Fig. 1 shows this with the approximate observational filter of GW vertical and horizontal wavelengths along with the altitude each instrument measures.

SOHIP was built by Lawrence Livermore National Laboratory (LLNL) to perform refractive stellar occultation of the stratosphere. The instrument utilizes hypertemporal imagers for high vertical resolution sampling of approximately 3 meters. However, the kilohertz frame rate for vertical sampling at a high resolution requires a bright star (or large signal strength for the stellar occultation), so the observations are limited to maximum of approximately 2 vertical profiles per orbit as the measurement is dependent on a bright star aligning with the limb-viewing line of sight. Thus, SOHIP observes vertical profiles sporadically for one-dimensional measurements in the vertical (z) dimension.

ECLIPSE and VvIPRE were built by Naval Research Laboratory (NRL) to measure radiance from the mesosphere through ionosphere. ECLIPSE performs both nadir and limb-view scanning with UV photometers for a 3D field measurement with both horizontal and vertical resolution of 10 km [3]. VvIPRE utilizes a limb view UV spectrograph observing 80 nm to 170 nm wavelength spectrum at a 10 km vertical resolution [4, 2]. ECLIPSE observes ion density in three dimensions by combining limb- and nadir-viewing instrument data while VvIPRE observes the emission spectrum in two dimensions (along-track and vertically) as it continually scans the vertical coordinate as the space station orbits.

AWE was built by Space Dynamics Laboratory at Utah State University to measure specific bands of the hydroxyl spectra with its nadir imager, observing vertically-averaged temperature between 78 km and 95.4 km altitudes with a horizontal resolution of 7.7 km and 20 km along-track and cross-track, respectively. The imager used by AWE has a

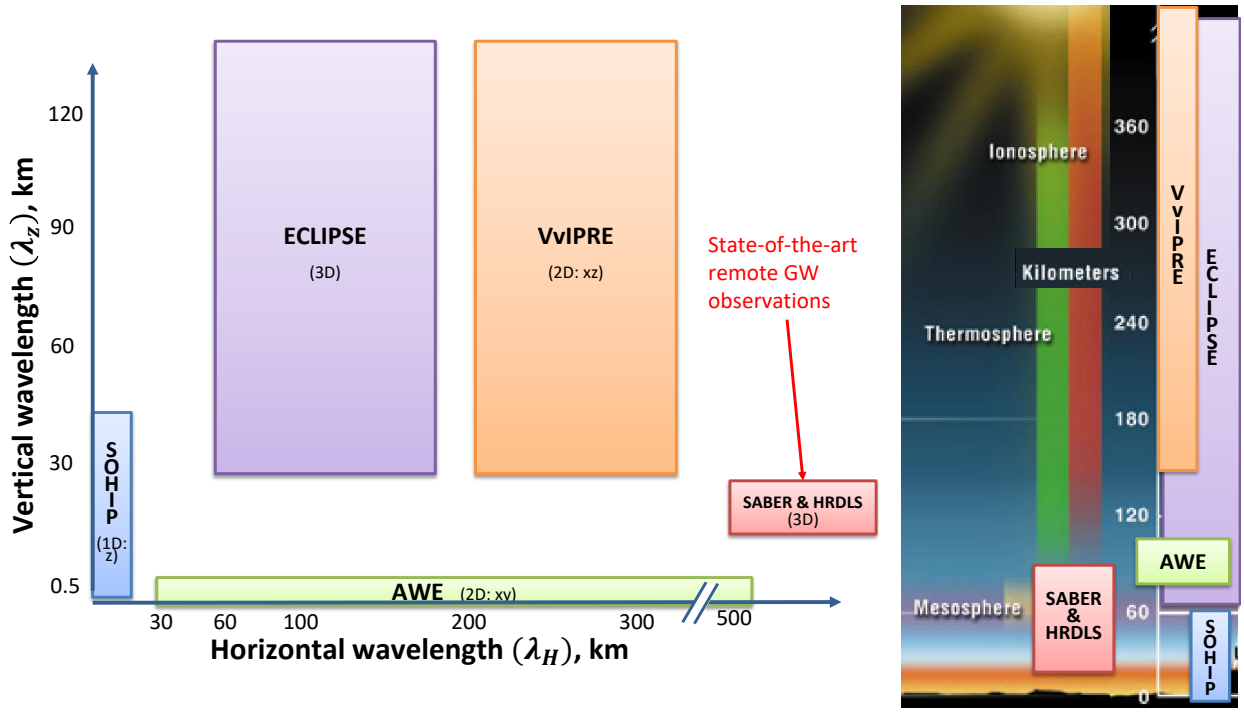

Fig. 1: Observational filter for the observable GW wavelengths by each of the four new ISS instruments compared with the state-of-the-art instruments SABER and HIRDLS.

field of view so that it observes two dimensions horizontally: along-track (x) and cross-track (y).

3. ATMOSPHERIC SIMULATIONS OF CONVECTIVE GRAVITY WAVES

This work investigates the feasibility of combining the ISS datasets with numerical atmospheric models for an Observing System Simulation Experiment (OSSE). However, due to the wide altitude range of the observations (10 km – 300 km and above), we utilize two atmospheric models. The GW generation and stratospheric propagation is simulated with the Weather Research & Forecasting (WRF) model. On the other hand, the medium scale traveling ionospheric disturbance (MSTID) due to a convective GW is simulated with SAMI3 (Sami3 is Also a Model of the Ionosphere).

3.1 Tropospheric and stratospheric simulation

The WRF model is a mesoscale model that simulates realistic or idealized weather [9]. This work uses WRF to simulate idealized convective GWs in a three-dimensional large eddy simulation. To simulate convective GWs, WRF is set up with 0.25 km vertical resolution and a domain that extends to roughly 70 km above ground with Rayleigh damping the top 10 km. The initial condition is a squall line at domain center from WK82 [10] and extended to higher altitudes with the empirical atmospheric model from NRL, NRLMSIS [5].

Fig. 2 shows the simulated convective GW in the troposphere and stratosphere six hours after initialization with the vertical wind speed three-dimensional field. After six hours, the GWs have propagated eastward (in the positive x-direction), as seen by the large vertical wind speed in the vertical plane.

3.2 Ionospheric disturbance simulation

SAMI3 is a global model solving ion continuity and momentum equations to predict plasma and evolution of ions from 100 km altitude developed by NRL. The model grid is aligned with Earth's geomagnetic field, and the ionosphere is driven by neutral atmosphere with forcing from below. In this work, we simulate MSTIDs from GWs generated by intense thunderstorms in Texas April 2014 at 08:00 – 10:30 UTC. The neutral atmosphere with convective GWs is simulated with the Whole Atmosphere Community Climate Model (WACCM) based on ionospheric observations of this real event [1].

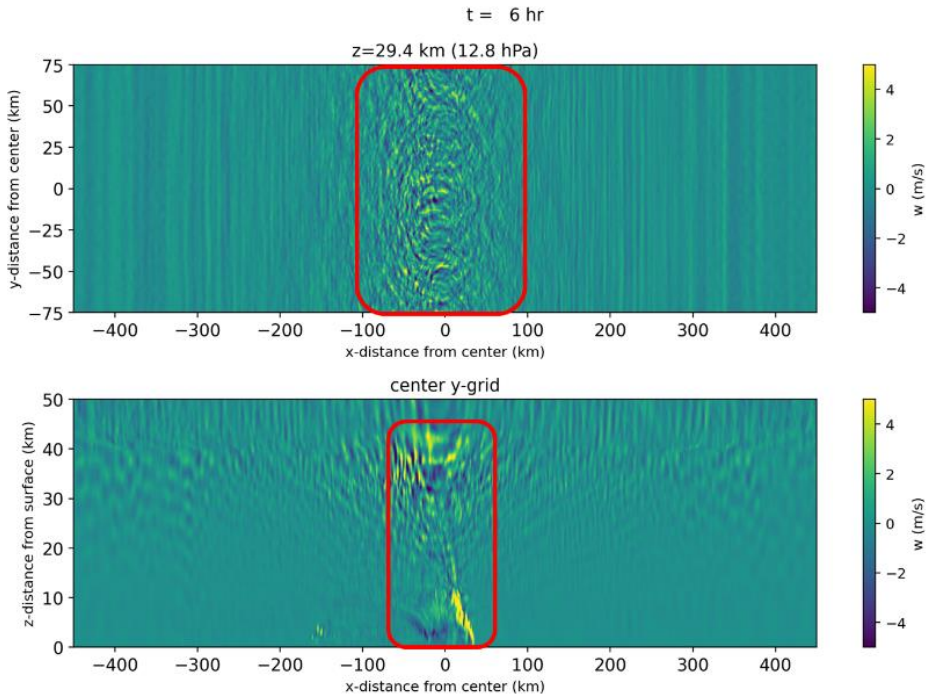

Fig. 2: Simulated vertical wind speed from an idealized WRF simulation with a squall line extending across the domain at center of the domain x-axis. Two-dimensional slices of the the wind field are shown with a horizontal plane at 29.4 km altitude in the top and a vertical plane at the domain center on the bottom. The source of convective GWs is highlighted with red rectangles.

4. SIMULATED MEASUREMENTS OF ISS INSTRUMENTS

To simulate a dataset from each instrument, we sample the model predictions at the instrument spatial resolution. Fig. 3 shows the ISS orbital track during the convective GW event in April 2014 along with the approximate propagation direction of the observed GWs.

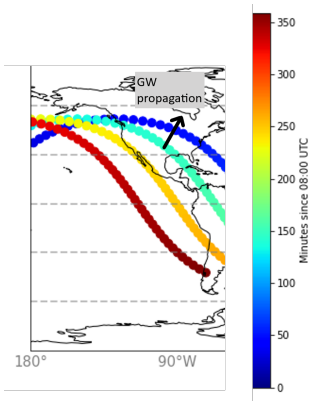

Fig. 3: Overpass time of the space station in minutes since initial convective storm observed over Texas, USA.

Since the ISS orbital path was almost exactly orthogonal to the GW propagation direction, we sample the model output along the propagation direction in the black arrow in Fig. 3 to assess the instruments' maximum observational potential. To characterize simulated observations from each instrument, we apply a one-dimensional Stockwell transform as a spectral analysis tool [6].

4.1 SOHIP

We simulate the SOHIP-observed GW from the WRF temperature vertical profile taken from center of domain, since SOHIP retrieves stratospheric temperature vertical profiles with stellar occultation. The vertical GW is the high-pass filtered temperature normalized by the low-pass filtered temperature profile. Fig. 4 shows this as the "true" GW in a black dashed. We utilized a model of instrument noise [7] to model 100 realizations of noisy synthetic measurements shown in solid color lines in Fig. 4.

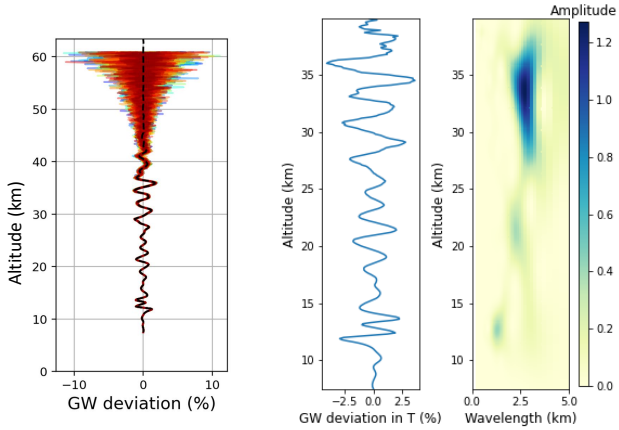

Fig. 4: Simulated GW measurements by SOHIP with 100 random noisy synthetic measurements from WRF shown in left panel. Spectral analysis of one simulated vertical GW observation by SOHIP shown in righthand two plots.

The Stockwell transform applied to one realization of the synthetic SOHIP measurements is shown in the righthand panels of Fig. 4. In this case, we observe vertical wavelengths between 1 km and 4 km with a wavelength increasing with altitude.

4.2 AWE

AWE measures mesospheric hydroxyl emissions to retrieve temperature at approximately 87 km altitude [8], so we take the neutral temperature horizontal field at 100 km altitude to approximate the AWE observations. We extract the GW deviations from a reference temperature field, which we estimate as the zonal mean temperature. Fig. 5 shows the simulated GW horizontal field at one timestamp on the left panels along with the approximate propagation path extracted for spectral analysis in a white dashed line.

The lower left panel in Fig. 5 shows the GW horizontal field sampled at 7.7 km and 20 km resolution in the east-west and north-south directions, respectiveily. AWE can observe GW at a higher resolution than the Sami3 model domain, but the instrument will not capture the entire horizontal field shown. The AWE field of view is 600 km wide so that only +/- 300 km from the nadir position is captured (e.g. from the white dashed line in this scenario).

Fig. 5 righthand panel shows the horizontal GW and wavelength extracted from the AWE synthetic measurements. If the ISS samples the GW along its propagation direction, AWE would measure a horizontal wavelength between 350 km and 1,000 km.

4.3 ECLIPSE

ECLIPSE observes the full three-dimensional field of ion density based on a tomographic reconstruction from the limb and nadir measurements of oxygen or magnesium ion densities, depending on if it is nighttime or daytime, respectively. Fig. 6 shows the horizontal GW based on oxygen ion density relative to the zonal mean field near 120 km altitude.

Similar to the AWE synthetic measurements, ECLIPSE samples the oxygen ion density at a higher resolution of 10 km compared with the Sami3 model domain. However the swath extent is +/- 400 km from the nadir point. This preliminary analysis only investigates one altitude level, but ECLIPSE would observer several other horizontal slices at a 10 km vertical resolution

The spectral analysis in the righthand panels of Fig. 6 show that ECLIPSE observes horizontal wavelengths between 450 km and 1,500 km at a 119 km altitude. ECLIPSE observes longer waves approximately 20 km above the AWE observations.

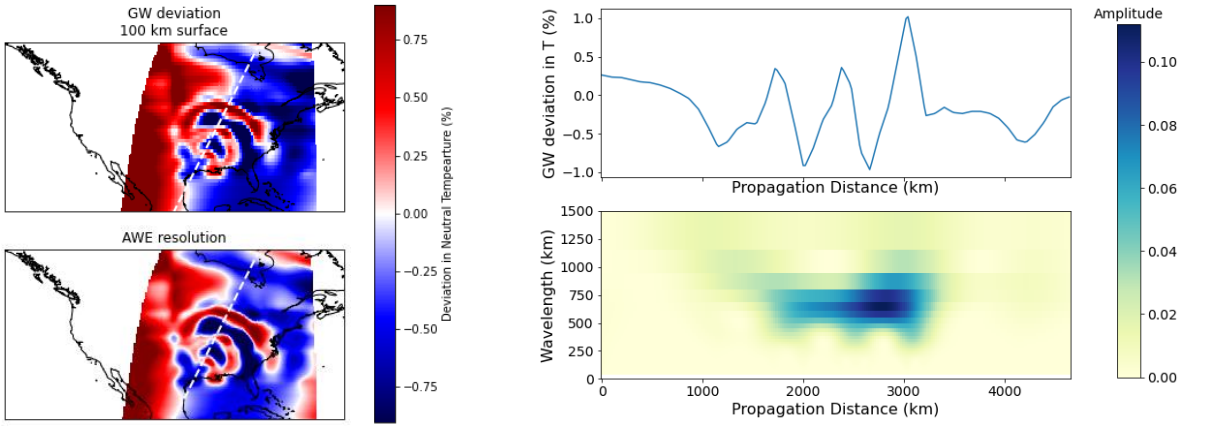

Fig. 5: Simulated GW field at altitude closest to AWE measurements from Sami3 neutral temperature. The left panel shows the 2D field with a white dashed line showing the section extracted for spectral analysis at the simulated and observed resolution in the top and bottom, respectively. The bottom left figure is interpolated to instrument resolution, which is finer than the Sami3 model grid shown in the upper left but the real instrument has a narrower field of view. The right panel shows the spectral analysis of simulated horizontal GW observation by AWE.

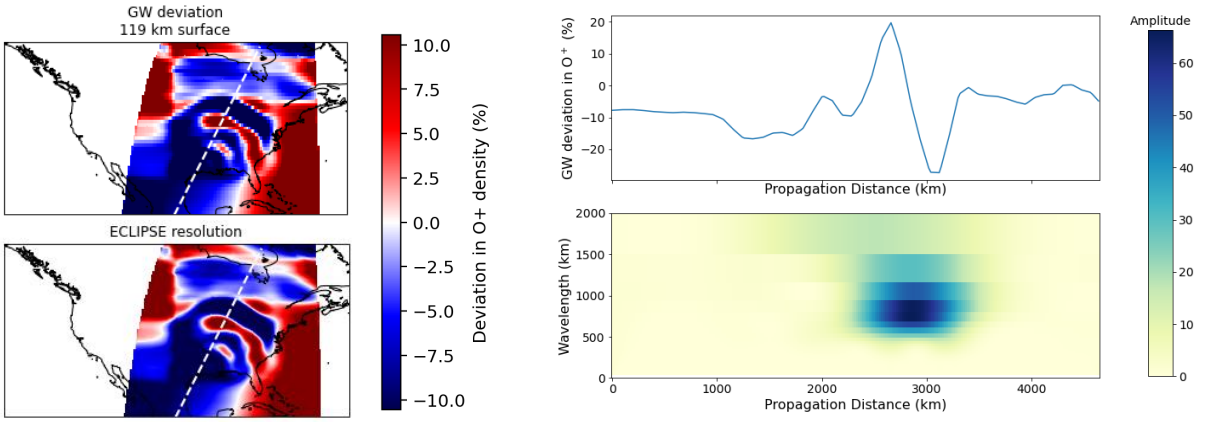

Fig. 6: Simulated GW field at an altitude near ECLIPSE measurements from Sami3 oxygen ion density. The left panel shows the 2D field with a white dashed line across the section extracted for spectral analysis. The right panel shows a spectral analysis of simulated horizontal GW observation by ECLIPSE.

4.4 VvIPRE

VvIPRE observes vertical profiles of the oxygen ion density with 10 km vertical resolution and a 90 second scan time leading to a horizontal resolution of approximately 200 km. For context, Fig. 7 shows the model predicted horizontal GW field at two altitudes on the left and right. In addition, the horizontal field is sampled on the VvIPRE along-track resolution of 200 km in the bottom panels of Fig. 7 along with the along-track section and the location used for a vertical spectral analysis in the white dashed lines and the star marker, respectively.

Since VvIPRE is a limb-viewing instrument, it only observes the atmosphere along-track and does not provide horizontal information during an orbit. Thus, due to its limited horizontal sampling and resolution, VvIPRE cannot observe the horizontal propagation of GWs.

Fig. 8 shows the vertical GW deviation in the oxygen ion density based on a reference profile from the average vertical profile along-track. The right panel of Fig. 8 shows a spectral analysis of the vertical profile scan at a propagation distance of 1600 km from the bottom of the domain shown in Fig. 7. The highest amplitude vertical wavelength observed is roughly 120 km at an altitude of 200 km.

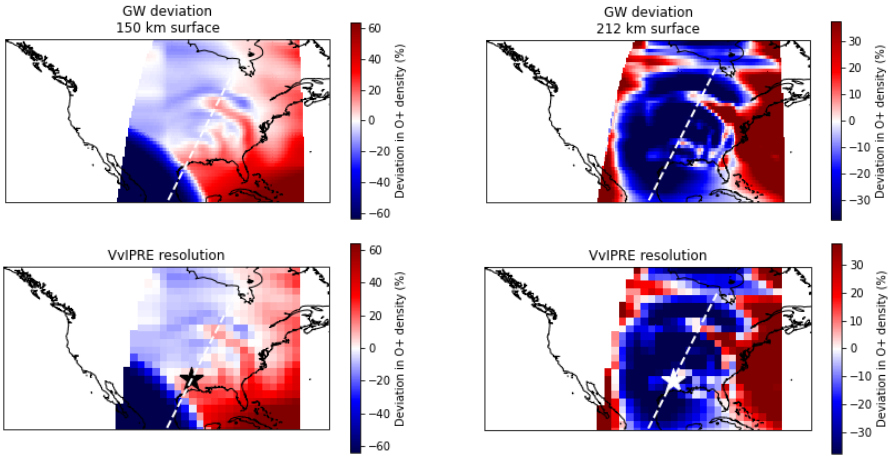

Fig. 7: Simulated GW horizontal plane shown at the native model resolution and at the VvIPRE along-track resolution in the upper and lower panels, respectively, from Sami3 oxygen ion density. The left panel shows the horizontal field at an altitude of 150 km and the right panel shows the field at a 212 km altitude.

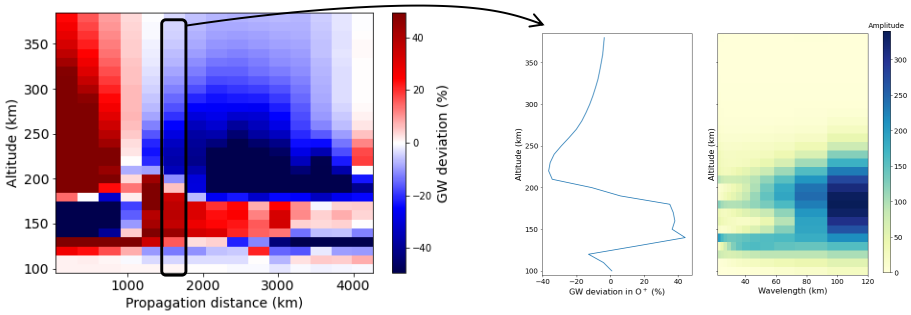

Fig. 8: Simulated GW vertical plane shown in left panel along the GW propagation direction sampled by VvIPRE from Sami3 oxygen ion density. The right panel shows the spectral analysis applied to the first scan at a 0 km distance.

The estimated GW deviation is strongly dependent on the reference vertical profile and this reference from VvIPRE measurements is not necessarily representative due to zonal deviations in the ion density. However, with ECLIPSE also measuring ion density horizontal fields, we can utilize those observations to inform the reference vertical profile and separate GW deviations from spatial variability.

5. SUMMARY AND FUTURE DIRECTIONS

This work utilizes atmospheric and space weather models to assess the ability of four new instruments on the International Space Station to characterize upper-atmosphere disturbances. The disturbances observed include turbulence below 60 km altitude and atmospheric gravity wave (GW) propagation from the troposphere to ionosphere. These observations have the potential to help validate a poorly constrained aspect of climate models: gravity wave drag.

In addition, three of the four ISS instruments assessed in this work were originally developed to deploy on CubeSats. These nano-satellites are at least 100 times cheaper and much quicker to launch than full-scale satellites, which offers the opportunity to launch multiple CubeSats to enable global coverage with higher spatial and temporal resolution.

Difficulties in combining data from these instruments includes the fact that the instruments are measuring different quantities (i.e., O+, neutral temperature) and observing different slices of the atmosphere. This analysis shows that SOHIP, ECLIPSE, and AWE will can observe GW propagation characteristics. The vertical propagation observed by VvIPRE spectrograph is also measured by ECLIPSE photometers, so the VvIPRE spectral measurements could

provide additional useful data on other ion densities.

The next steps toward observing GWs from the space station includes applying more rigorous 2-dimensional spectral analysis for analyzing horizontal wavelengths and propagation direction. In addition, we need to assess the temporal sampling of atmospheric waves to better understand observable wave timescales. Gaps between different datasets can also be filled by utilizing the wave dispersion relationship.

Observations from SOHIP could provide corrections for ground-based space object imaging as turbulence distorts the captured images. Additionally, GWs may impact electromagnetic wave propagation degrading navigation systems. Both of these Space Situational Awareness issues can be mitigated with knowledge on the characteristics, spatial, and temporal distribution of GWs and turbulence.

6. ACKNOWLEDGMENTS

We would like to acknowledge Mike Taylor and Jeff Forbes for useful discussions and advice on the AWE instrument. This work was performed under the auspices of the U.S. Department of Energy by Lawrence Livermore National Laboratory under Contract DE-AC52-07NA27344 with IM release number LLNL-CONF-853767. This work was funded by Laboratory Directed Research and Development Feasibility Study project "Remote Observation of Gravity Waves with Multiple Satellite Datasets" with tracking code 23-FS-06.

7. REFERENCES

[1] Irfan Azeem, Jia Yue, Lars Hoffmann, Steven D. Miller, William C. Straka III, and Geoff Crowley. Multisensor profiling of a concentric gravity wave event propagating from the troposphere to the ionosphere. *Geophysical Research Letters*, 42(19):7874–7880, 2015.

[2] S. A. Budzien, K. F. Dymond, B. A. Fritz, A. C. Nicholas, A. W. Stephan, and E. J. Wagner. The variable voltage ion protection experiment (VVIPRE): Thermospheric and ionospheric remote sensing from the iss. In *Ionospheric Effects Symposium 2023 (IES2023)*, Alexandria, VA, USA, 2023.

[3] K. F. Dymond, A. C. Nicholas, B. A. Fritz, S. A. Budzien, A. W. Stephan, C. M. Brown, E. J. Wagner, M. R. Burleigh, D. P. Drob, and K. A. Zawdie. The experiment for characterizing the lower ionosphere and prediction sporadic-e (ECLIPSE) missions: Instruments to study the dynamics of the lower ionosphere. In *Ionospheric Effects Symposium 2023 (IES2023)*, Alexandria, VA, USA, 2023.

[4] K. F. Dymond, A. C. Nichols, S. A. Budzien, C. Coker, A. W. Stephan, and D. H. Chua. The special sensor ultraviolet limb imager instruments. *J. Geophys. Res. Space Physics*, 122:2674–2685, 2017.

[5] J. T. Emmert, D. P. Drob, J. M. Picone, D. E. Siskind, M. Jones Jr., M. G. Mlynczak, P. F. Bernath, X. Chu, E. Doornbos, B. Funke, L. P. Goncharenko, M. E. Hervig, M. J. Schwartz, P. E. Sheese, F. Vargas, B. P. Williams, and T. Yuan. NRLMSIS 2.0: a whole-atmosphere empirical model of temperature and neutral species densities. *Earth and Space Science*, 8(3):e2020EA001321, 2021.

[6] A. Gramfort, M. Luessi, E. Larson, D. Engemann, D. Strohmeier, C. Brodbeck, R. Goj, M. Jas, T. Brooks, L. Parkkonen, and M. Hämäläinen. MEG and EEG data analysis with MNE-Python. *Frontiers in Neuroscience*, 7, 2013.

[7] D. L. McGuffin, P. J. Cameron-Smith, M. A. Horsley, B. J. Bauman, W. De Vries, D. Healy, A. Pertica, C. Shaffer, and L. M. Simms. Stratospheric temperature measurements from nanosatellite stellar occultation observations of refractive bending. *Atmospheric Measurement Techniques*, 16(8):2129–2144, 2023.

[8] P.-D. Pautet, M. J. Taylor, W. R. Pendleton, Y. Zhao, T. Yuan, R. Esplin, and D. McLain. Advanced mesospheric temperature mapper for high-latitude airglow studies. *Appl. Opt.*, 53(26):5934–5943, Sep 2014.

[9] W. C. Skamarock, J. B. Klemp, J. Dudhia, D. O. Gill, Z. Liu, J. Berner, W. Wang, J. G. Powers, M. G. Duda, D. M. Barker, and X.-Y. Huang. A description of the Advanced Research WRF Version 4. Technical report, NCAR, 2019. NCAR/TN-556+STR.

[10] M. L. Weisman and J. B. Klemp. The dependence of numerically simulated convective storms on vertical wind shear and buoyancy. *Monthly Weather Review*, 110:504–520, 1982.